VCAM-1 Secreted from Cancer-Associated Fibroblasts Enhances the Growth and Invasion of Lung Cancer Cells through AKT and MAPK Signaling

Zhuan Zhou, Qin Zhou, Xia Wu, San Xu, Xiaohong Hu, Xuxiu Tao, Bo Li, Jinwu Peng, Dan Li, Liangfang Shen, Ya Cao, Lifang Yang

PII: S0304-3835(19)30661-5

DOI: https://doi.org/10.1016/j.canlet.2019.12.039

Reference: CAN 114635

To appear in: *Cancer Letters*

Received Date: 20 September 2019

Revised Date: 19 December 2019

Accepted Date: 20 December 2019

Please cite this article as: Z. Zhou, Q. Zhou, X. Wu, S. Xu, X. Hu, X. Tao, B. Li, J. Peng, D. Li, L. Shen, Y. Cao, L. Yang, VCAM-1 Secreted from Cancer-Associated Fibroblasts Enhances the Growth and Invasion of Lung Cancer Cells through AKT and MAPK Signaling, *Cancer Letters*, https://doi.org/10.1016/j.canlet.2019.12.039.

Abstract

Several studies have indicated that cancer-associated fibroblasts (CAFs) could promote tumor progression in many malignancies. However, the mechanism by which CAFs promote the growth and metastasis of lung cancer remains poorly defined. In the present study, CAFs and normal fibroblasts (NFs) were isolated from human lung cancer and adjacent tissue. The data showed that the conditional medium (CM) of CAFs could increase the proliferation, migration and invasion of lung cancer cells. Vascular cell adhesion molecule-1 (VCAM-1) showed a higher expression in CAF-CM than NF-CM, and blocking VCAM-1 in CAF-CM attenuated the proliferation and invasion of cancer cells. Further, the results showed that VCAM-1 secreted from CAFs activated AKT and MAPK signaling via receptor α4β1 integrin (very-late antigen (VLA)-4) in lung cancer cells. Moreover, CAFs promoted VCAM-1 expression and tumor growth in vivo. Additionally, bioinformatics analysis indicated a positive correlation on the CAF marker protein alpha-smooth muscle actin (α-SMA) and VCAM-1 expression, which was associated with a poor prognosis in cancer patients. These findings demonstrate that the VCAM-1 secreted from CAFs enhances growth and invasion by activating the AKT and MAPK signaling of lung cancer cells.

VCAM-1 Secreted from Cancer-Associated Fibroblasts Enhances the Growth and Invasion of Lung Cancer Cells through AKT and MAPK Signaling

Zhuan Zhou[a,b,1], Qin Zhou[a,1], Xia Wu[a,b], San Xu[a,b], Xiaohong Hu[c], Xuxiu Tao[a,b], Bo Li[d], Jinwu Peng[d], Dan Li[c], Liangfang Shen[a], Ya Cao[a,b], Lifang Yang[a,b,*]

[a] Departments of Oncology, Key Laboratory of Carcinogenesis and Cancer Invasion of Ministry of Education, Xiangya Hospital, Central South University, Changsha 40078, China;

[b] Cancer Research Institute, School of Basic Medicine Science, Central South University, Changsha 410078, China;

[c] Institute of Molecular Medicine and Oncology, College of Biology, Hunan University, Changsha 410082, China;

[d] Pathology Department, Xiangya Hospital, Central South University, Changsha 410078, China;

[*]**Correspondence:** Central South University, Xiangya Road 110, Changsha 410078, China. Email address: yanglifang@csu.edu.cn (L.Yang)

[1]These authors contributed equally to this work.

Abstract

Several studies have indicated that cancer-associated fibroblasts (CAFs) could promote cancer progression in many malignancies. However, the mechanism by which CAFs promote the growth and metastasis of lung cancer remains poorly defined. In the present study, CAFs and normal fibroblasts (NFs) were isolated from human lung cancer and adjacent tissue. The data showed that the conditional medium (CM) of CAFs could increase the proliferation, migration and invasion of lung cancer cells. Vascular cell adhesion molecule-1 (VCAM-1) showed a higher expression in CAF-CM than NF-CM, and blocking VCAM-1 in CAF-CM attenuated the proliferation and invasion of cancer cells. Further, the results showed that VCAM-1 secreted from CAFs activated AKT and MAPK signaling via receptor α4β1 integrin (very-late antigen (VLA)-4) in lung cancer cells. Moreover, CAFs promoted VCAM-1 expression and tumor growth in vivo. Additionally, bioinformatics analysis indicated a positive correlation on the CAF marker protein alpha-smooth muscle actin (α-SMA) and VCAM-1 expression, which was associated with a poor prognosis in cancer patients. These findings demonstrate that the VCAM-1 secreted from CAFs enhances growth and invasion by activating the AKT and MAPK signaling of lung cancer cells.

Key words: Cancer-associated fibroblasts; Vascular cell adhesion molecule-1; AKT, MAPK, Cancer invasion

1. Introduction

Lung cancer is the leading cause of cancer death and exhibits the highest morbidity and mortality globally, the overall 5-year survival rate is 15% [1, 2]. Most lung cancer patients die of metastasis, thus, understanding the mechanism of lung cancer metastasis is urgently needed[3]. Recent studies have shown that cancer progression and metastasis are not only associated with the properties of tumor cells, but also depend on the tumor microenvironment (TME)[4]. Among the stromal cells of TME, cancer-associated fibroblasts (CAFs) are a dominant component, exhibiting a classic spindle-shape morphology with a potential for planar polarity and over-expression of marker proteins including alpha-smooth muscle actin (α-SMA) and fibroblast-activated protein (FAP)[5, 6]. Accumulating research has demonstrated that cancer cells can establish cross-talk with CAFs to enhance tumor metastasis[7], and a strong association between CAFs and poor prognosis has been shown in several types of cancer, including lung cancer[8-10].

CAFs can secrete cytokines, growth factors, CAF-specific proteins and exosomes to support cancer cell growth, metastasis and confer chemoresistance to lung cancer[11, 12]. CAFs support the growth of lung cancer cells in vivo by the secretion of the cytokines cardiotrophin-like cytokine factor 1 (CLCF1) and IL6 that directly stimulate the growth of cancer cells[13], IL-22 secreted from CAFs significantly increases the proliferation, migration and invasion of lung cancer cells but reduces apoptosis via the activation of PI3K-Akt-mTOR signaling[14]. A subset of CAFs, CD90 (+) CAFs, secrete insulin-like growth factor-II (IGF-II) activated IGF1R signaling in cancer cells, induce nanog expression and promote stemness[15]. Also, IGF-1 and hepatocyte growth factor(HGF), secreted by CAFs, synergistically induce Annexin A2(ANXA2) expression, thus promoting epithelial–mesenchymal transition (EMT) and drug resistance in non-small cell lung cancers (NSCLCs) [16]. Recent research has found that CAFs deliver SNAIL1 to recipient cells via exosomes and induce EMT in lung cancer cells[17].

To better understand the mechanism of the interaction of CAFs with lung cancer cell in growth

and invasion, the current study demonstrated that CAF-conditional medium (CM) enhanced the proliferation and invasion of the recipient cancer cells. Interestingly, we found that vascular cell adhesion molecule-1 (VCAM-1), secreted from CAFs, was upregulated compared with the normal fibroblasts (NFs), and blocking the expression of VCAM-1 in CAFs led to the attenuation of the proliferation and invasion of cancer cells. Moreover, we verified that VCAM-1 secreted from CAFs activated the AKT and MAPK pathway via a receptor, the α4β1 integrin (also known as very-late antigen, VLA-4) in cancer cells. In vivo, we proved that VCAM-1 increased tumor growth. Collectively, the present work provides solid evidence that VCAM-1, secreted from CAFs, enhances the growth and invasion of lung cancer cells, implying that VCAM-1 may be a potential anti-metastasis therapeutic target of lung cancer.

2.Material and methods

2.1 Cell culture and reagents

A549 and H358 cells were obtained from the American Type Culture Collection (ATCC, Manassas, VA, USA). A549 was cultured in DMEM/F12 (Gibco BRL, Gaithersburg, MD, USA) supplemented with 10% fetal bovine serum (FBS, Hyclone, Logan, UT, USA), and H358 cells were cultured in RPMI 1640 (Gibco BRL) supplemented with 10% FBS at 37 °C in a 5% CO_2 incubator. Recombinant human VCAM-1(150-04-100) was obtained from Peprotech (USA). VCAM-1(AF809) and Sheep IgG (5-001-A) were purchased from R&D system (Minneapolis, MN, USA).

2.2 Primary cell culture

Primary CAFs and NFs were isolated from lung cancer and adjacent normal tissues of three patients who underwent surgical resection in 2016 at the Xiangya hospital, Central South University. The patients did not receive chemotherapy or radiation therapy before surgery. The collection of specimens was approved by the Ethics Committee of Xiangya Hospital, and informed consent was obtained from all the patients. Fibroblasts were isolated as previously described [18]. Briefly, fresh tissues were minced with surgical blades to dissect off unwanted tissue (fat, necrotic material) and chopped finely with crossed scalpels to about 1 mm cubes in 5

ml of sterile phosphate buffer saline (PBS, with 1% penicillin and streptomycin). Tissue fragments were digested with 160 μg/ml collagenase A (Sigma Aldrich, St Louis, MO, USA) and 25 μg/ml hyaluronidase (Sigma Aldrich) for 2 hours at 37 °C. Then, they were seeded in a T25 culture flask with 5 ml of RPMI-1640 medium containing 10% FBS. The culture medium was changed after 48 hours to remove unattached cells and debris in suspension. Attached cells were cultured for 7–10 days to 1×10^6 cells. Conditioned media (CM) were obtained from 48-hour serum-starved cells and preserved at -80 □.

2.3 Cell viability assay

Cell viability was measured by MTS kit (G5421, Promega, Madison, WI, USA) following the manufacturer's instruction. Lung cancer cells were cultured in a 96-well plate with CAF-CM or NF-CM for the indicated time, and then the assay solution was added for an incubation of 1.5 hours under conditions away from light. The Microplate Reader (BioTek ELx800, Winooski, VT, USA) was used to measure the results at 490 nm.

2.4 Wound healing assay.

Cells grew to 80% confluence in a 24-well plate and were wounded by making a single scratch in the monolayer with a sterile 200 μl pipette tip, followed by a wash with 1× PBS to remove detached cells. The culture medium was then replaced with CAF-CM or NF-CM for the appropriate time. Photographs of the same area of the wound were taken at 100× magnification using a phase-contrast microscope.

2.5 Cell invasion assay

Lung cancer cell invasion assay was conducted using 24-well Matrigel-coated Transwell inserts (BD Biosciences, San Diego, CA, USA). Cells were trypsinized and re-suspended in serum-free medium and seeded at 2×10^5 cells in 0.2 ml medium to the upper chamber. Next, 0.8 ml CAF-CM or NF-CM was added to the lower chamber, and after incubation at 37 ℃ with 5% CO_2 for an appropriate time, the cells were stained with 0.1% crystal violet solution. The cells and Matrigel on the top surface of the filter were carefully removed with a cotton swab. The invasive cells attached to the bottom surface of the filter were quantified under a light microscope (×200).

The data are presented as the average number of cells from randomly chosen fields. Each treatment condition was assayed using triplicate filters, and all filters were counted in five areas.

2.6 Cytokine Antibody Arrays

A Human Cytokine Antibody Arrays kit (ARY022B, R&D system, Minneapolis, MN, USA) was used according to the manufacturer's instructions. Briefly, the arrays were blocked, incubated with 100 μl of condition medium overnight, followed by biotin-conjugated antibodies incubation for 2 hours and by HRP-linked secondary antibody for 1 hour. Luminescence analysis of membranes was visualized with an enhanced chemiluminescence detection kit (Pierce, Rockford, IL, USA), and quantitative array analysis was performed using ImageJ software (National Institutes of Health, Bethesda, Maryland, USA).

2.7. Enzyme-linked immunosorbent assay (ELISA)

The levels of soluble VCAM-1 in the supernatant of primary cell and cancer cell and the plasma VCAM-1 level of xenograft mice were measured by human VCAM-1 ELISA kit (EK0537, Boster, China), according to the manufacturer's instructions. The absorbance (450 nm) of each sample was detected on a standard automatic microplate reader (BioTek, USA).

2.8 Quantitative RT-PCR

Total RNA was obtained with total RNA purification (15596026, Thermo Fisher Scientific, Waltham, MA, USA) and reverse transcription (K1621, Thermo Fisher Scientific) according to the manufacturer's instructions. Quantitative PCR was performed with SYBR Green (4309155, Life technologies corporation, Gaithersburg, MD, USA) using an ABI 7500 instrument (Foster city, CA, USA). The primers are listed in Table1.

2.9 Western blotting analysis

Proteins were extracted from cells in IP lysis buffer (87787, Thermo Fisher Scientific) with a cocktail (4693116001, Roche, Basel, Switzerland) and PhosStop (4906845001, Roche). Total cell lysates were denatured in sodium dodecyl sulfate (SDS, Sigma-Aldrich) loading buffer and boiled for 5 minutes. Samples were separated by SDS-polyacrylamide gel electrophoresis (SDS-PAGE)

and transferred to polyvinylidene fluoride (PVDF) membranes (Merck Millipore, Billerica, MA, USA). Membranes were blocked with 5% milk in Tris-buffered saline–Tween 20 (TBST) and incubated overnight at 4 °C with primary antibodies. Membranes were then washed and incubated with appropriate horseradish peroxidase-conjugated secondary antibodies for 1 hour at room temperature. Membranes were washed again, and bands were visualized with enhanced chemiluminescence detection kit (Pierce).The α-SMA (NB-600-531, 1:1000), FAP (NB-110-8534, 1:100) and Vimentin (NBP1-31327, 1:1000) antibodies were purchased from Novus Biologicals(Littleton,CO,USA);PDFGR-α(3174,1:1000),P38(8690,1:1000),p-P38 (thr180/try182,4511,1:1000) , AKT (9272,1:1000), ERK (4695,1:1000), p-ERK1/2 (4370, 1:1000), p-JNK (9251,1:1000), anti-rabbit IgG-HRP (14708,1:2000) and anti-mouse IgG-HRP (14709,1:2000) antibodies were obtained from Cell signaling technology (Danvers, MA, USA); JNK (SAB4200176,1:1000) antibody was purchased from Sigma-Aldrich; p-Akt (ser473, 66444-1-IG,1:2000), VLA-4 (26918-1-AP,1:1000), VCAM-1(11444-1-AP,1:500) antibodies were purchased from Proteintech (Chicago, IL, USA); Bcl-2 (7382,1:500) antibody was obtained from Santa Cruz Biotechnology (Santa Cruz, CA, USA); β-actin (AC026) antibody was purchased from ABclonal (Wuhan, China).

2.10 RNA interference

The small interfering RNA (siRNA) transfected into A549 and H358 cells was Lipofectamine 2000 reagent (Invitrogen, Carlsbad, CA, USA), and the final concentration of siRNA was 100 nmol/L. VLA-4 siRNA-1: 5'-GGCUCCAAAGAUAUAAAGATT-3'(forward); 5'-UCUUUAUA UCUUUGGAGCCTT-3' (reverse); siRNA-2:5'-GCCUUCAAUAAAGGAGAAATT-3' (forward); 5'-UUUCUCCUUUAUUGAAGGCTT-3'(reverse); siRNA-3:5'-GGAGUUUGCUAAAUUUGA ATT-3'(forward); 5'-UUCAAAUUUAGCAAACUCCTT-3'(reverse); and negative control siRNA 5'-UUCUCCGAACGUGUCACGUTT -3' (forward); 5'–UUCAAAUUUAGCAAACUCCTT-3'(reverse) were purchased from Gene Pharma (Suzhou, China).

2.11 Animal experiments

All mice were maintained and manipulated according to guidelines established by the Medical Research Animal Ethics Committee of Central South University. The mixture of 2×10^6 H358

cells with 5×10^5 NFs or 5×10^5 CAFs cells (4:1) was re-suspended in 100 μl PBS and injected subcutaneously into six-week-old female athymic nude mice (BALB/C) as previously described [19]. Tumor formation was examined every 3 days. The tumor volume was calculated as volume(mm^3) = $d^2 \times D/2$, where d and D were the shortest and the longest diameters, respectively. When tumor volume reaching to 60-80 mm^3, anti-VCAM-1 or IgG were intraperitoneally injected into mice at 50 mg/kg every 3 days for 5 times [20]. At the indicated time points, animals were sacrificed, blood collection was used to measure the plasma VCAM-1 level, and tissues were collected and fixed with 10% buffered formalin for immunohistochemistry (IHC) analysis.

2.12 Immunohistochemistry (IHC)

Immunohistochemistry was performed using a Histomouse SP Broad Spectrum DAB kit (Invitrogen–Zymed, Carlsbad, CA). After treating with 3% H_2O_2, the sections were blocked with 10% goat normal serum, and incubated with appropriate primary antibodies overnight at 4 °C. Then, the sections were sequentially incubated with biotin anti-mouse/rabbit IgG for 10 minutes and streptomyces anti-biotin-peroxidase for 10 minutes and stained with DAB for 1–3 minutes. All immunostained sections were then lightly counterstained with Mayer hematoxylin.

2.13 Bioinformatics analysis

The gene expression profiles GSE30219 were from the Gene Expression Omnibus database[21]. Survexpress was utilized to obtain the relationship between the expression of α-SMA, VCAM-1, ITGA4(VLA-4α), ITGB1(VLA-4β) and disease risk. The relevance of α-SMA /VCAM-1, VCAM-1/ITGA4(VLA-4α), VCAM-1/ ITGB1(VLA-4β) in lung cancer patients was evaluated by Pearson correlation analysis. Survexpress was also employed to analyze the expression of VCAM-1 on the overall survival among lung cancer patients. The clinical and pathological features and VCAM-1 expression of patients are shown in Table 2.

2.14 Statistical analysis

Data analysis was conducted by the SPSS software (version 21.0; SPSS). Statistical differences were determined using Student's t-test. All values are expressed as mean values ± S.E. of three individual experiments. A value of $p < 0.05$ was considered statistically significant.

3. Results

3.1 The conditional medium (CM) of CAFs promotes the proliferation, migration and invasion of recipient lung cancer cells

Primary cells were isolated from lung cancer and adjacent normal tissues of three patients. Consistently with previous reports[3], the morphology of the two primary cells is a long-spindle shape, suggesting that these cells were fibroblasts (Figure.1A). Western blotting analysis results indicated that more α-SMA and FAP were expressed in CAFs than NFs in three paired primary cultured cells (Figure.1B). Meanwhile, α-SMA, FAP and PDFGR-α of CAFs were higher than two generation NFs (NFs-P2), and the mesenchyme marker vimentin has an equal expression level in these two cells (Figure.1C). This indicated that the primary cultured fibroblasts are CAFs and NFs. In the process of cell subculture in vitro, due to the presence of some cytokines in the culture serum, NFs could be transformed into CAFs [22]. For this reason, the data also indicated that α-SMA expression levels could be increased to their level in CAF when NF was subcultured to eighth generations, implying the trend of activation (Figure.1D). For the reliability of the experiments, we used NFs from ≤sixth generations of NFs in the following research.

To explore the effect of CAFs on lung cancer cells, we cultured A549 and H358 cells with the CAF-CM and NF-CM, respectively. The viability assay showed that both A549 and H358 cultured with CAF-CM could enhance the proliferation of cancer cells more than NF-CM after 48 and 72 hours (Figure. 1E). Moreover, the data of the wound healing assay showed that both A549 and H358 cells cultured with CAF-CM for 48 hours had a more significant migration ability than that of NF-CM ($p < 0.01$) (Figure. 1F). Further, transwell assay was performed to test the invasion ability of A549 and H358 cells. As shown in Figure 1G, compared with NF-CM, CAF-CM dramatically increased the invasion of lung cancer cells after 48 hours ($p < 0.01$ and $p < 0.001$, respectively). These data indicate that CAF-CM can promote the proliferation, migration and invasion of recipient lung cancer cells.

3.2 Identification of differentially secreted cytokines between CAF-CM and NF-CM

To identify cytokines secreted by CAFs that play a key role in the proliferation and invasion of lung cancer cells, we collected the CM from two paired CAFs and NFs, respectively, and

performed a cytokine antibody array analysis, the immunoblot results showed that 11 cytokines were highly expressed in CAF-CM compared with NF-CM, including angiogenin, cystatin C, CD147, HGF, IGFBP-2, IGFBP-3, MIF, SDF-1, TBSN, VEGF, and VCAM-1($p < 0.01$) (Figure 2A,B). Among these, HGF, VEGF and VCAM-1 were obviously upregulated ($p < 0.001$). Then, the mRNA expression levels in CAFs and NFs were verified by quantitative RT-PCR. It was found that the expression of VCAM-1 in CAF was the highest (Figure.2C). Further, ELISA assay results showed that the concentration of soluble VCAM-1 was higher in the CAF-CM than in NF-CM ($p < 0.001$) (Figure. 2D). Taken together, VCAM-1 may be an important cytokine for CAF to perform its biological functions in lung cancer through the paracrine pathway.

3.3 CAFs promote the proliferation, migration and invasion of lung cancer cells via the secretion of VCAM-1

To further explore the role of VCAM-1in the process of CAFs promoting the proliferation, migration and invasion of lung cancer cells, viability, wound healing and transwell assays were performed using lung cancer cells co-cultured with NF-CM, CAF-CM, CAF-CM+IgG and CAF-CM+VCAM-1 antibodies which could block the expression of VCAM-1 in CAF-CM. Meanwhile, there is a certain degree of VCAM-1 expression in CM of cancer cells, but it is significantly lower than in CM of CAF (Figure.3A). Consistent with the results in Figure 1, the data of the viability assay showed that both A549 and H358 cell proliferation was enhanced more in CAF-CM than in NF-CM. Further, the data indicated that the proliferation of A549 and H358 cells was remarkably decreased when blocking the VCAM-1 expression in CAF-CM using VCAM-1 antibody ($p < 0.001$) (Figure.3B). Moreover, the wound healing assay results suggested that anti-VCAM-1 antibody could also attenuate the migration of A549 and H358 cells cultured with CAF-CM ($p < 0.05$ and $p < 0.001$, respectively) (Figure.3C). To demonstrate the role of VCAM-1 on CAF-driven cancer cell invasion, as shown in Figure.3D, compared with the CAF-CM+IgG group, adding anti-VCAM-1 antibody could drastically decrease the invasion ability of lung cancer cells ($p < 0.01$and $p < 0.001$, respectively).

As a secreted protein, recombinant human VCAM-1 was used to assess the effect of VCAM-1 on the proliferation, migration and invasion of lung cancer cells. The proliferation of A549 and H358 cells were increased in a dose-dependent manner in response to VCAM-1 ($p < 0.001$) (Figure.3E).

Simultaneously, in the migration and invasion experiments, VCAM-1 drastically facilitated the migration and invasion of A549 and H358 (Figure.3F, G). These data indicate that VCAM-1 is a critical cytokine in CAF-CM which can promote lung cancer cell proliferation, migration and invasion.

3.4 CAF-derived VCAM-1 activates the AKT, JNK and P38 pathway via receptor VLA-4

Previous studies have demonstrated that VCAM-1 is involved in promoting cancer metastasis in some cancers, including lung cancer[23], and VCAM-1 mediated the cancer metastasis mainly depending on the binding receptor VLA-4 and further activates the PI3K/AKT[24], MAPK[25, 26], Bcl-2[27] and ERK[28] pathways. In the present study, firstly, we analyzed which signaling pathway of lung cells activated by VCAM-1 was derived from CAFs. As shown in Figure 4A, after culturing A549 and H358 cells with CAF-CM, compared with the NF-CM group, the CAF-CM could induce the upregulation of the phosphorylation of AKT, JNK and P38, which gradually increased as the treatment time is increased from 1 day to 3 days, but this did not change the levels of total AKT, JNK and P38. However, CAF-CM has no influence on Bcl-2 in A549 and H358 cells. Meanwhile, the phosphorylation of ERK was gradually increased in A549 cells, and the expression of total ERK exhibited similar changes. However, the opposite results were observed in H358 cells. These results suggested CAFs mainly activate AKT and MAPK signaling pathways in lung cancer cells. We then analyzed whether CAFs activate AKT and MAPK signaling through VCAM-1/VLA-4 pathways. As shown in Figure.4B, C, there are VLA-4 protein expression in cancer cells, and upregulation of VLA-4 in A549 and H358 cells was induced by exogenous VCAM-1 in a dose-dependent manner. Simultaneously, the JNK, AKT, P38 signaling pathway was also activated. To further analyze the role of the VLA-4 receptor in the VCAM-1-mediated signaling pathway, we used siRNA to knock down the VLA-4 expression of recipient lung cancer cells. Quantitative RT-PCR and Western blot results indicated that the all three target VLA-4 siRNAs had an obvious inhibitory effect (Figure.4D, E). Furthermore, the inhibition of VLA-4 could reduce the phosphorylation of AKT, JNK and P38, and no significant difference was shown in the total AKT, JNK and P38 in A549 and H358 cells after being cultured with CAF-CM for 3 days (Figure.4F). Taken together, these findings suggest that CAF activates AKT and MAPK signaling pathways in lung cancer cells via the VCAM-1/VLA-4 axis.

Next, we investigated whether VLA-4 is involved in VCAM-1-mediated cancer cell progression. As results shown in Figure.5A, the promoting effect of CAF-CM on cancer cell growth was remarkably decreased when VLA-4 was knockdown using siRNA in cancer cell ($p < 0.001$). And the facilitating effect of CAF-CM on A549 and H358 cell migration and invasion was predominantly abrogated in the cancer cells with VLA-4 knockdown ($p < 0.001$) (Figure.5B, C). Hence, these data further confirm that VCAM-1-mediated VLA-4 involves in cancer cell progression.

3.5 VCAM-1 secreted from CAFs enhances tumor growth in vivo

To further investigate whether CAFs stimulate tumor progress in vivo, we co-cultured the H358 cells and CAFs or NFs at a ratio of 4:1, and then subcutaneously inoculated them into the nude mice to establish the xenograft tumor, followed by the treatment of VCAM-1Ab. As shown in Figure 6A, B, the tumor volumes of H358 cells in the CAFs group were exclusively larger than those of H358 cells in the NFs group, and these were 2–3-fold larger than H358 cells in the NFs group after 4 weeks ($p < 0.001$). And treatment with a VCAM-1 neutralizing antibody blocked the stimulatory effects of CAFs on the xenograft tumor growth in vivo ($p < 0.001$). The tumor weights of H358 cells with CAFs were also heavier than of H358 cells with NFs ($p < 0.01$), and the VCAM-1 antibody group showed more significant decrease of the xenograft tumor weight than control group ($p < 0.01$) (Figure.6C). Meanwhile, there was no significant difference in mice body weight between the four groups (Figure.6D). Moreover, co-inoculation of CAFs and H358 cells promote the plasma VCAM-1 level, which could be effectively inhibited by VCAM-1 antibodies ($p < 0.01$) (Figure.6E). Further, the IHC analysis of tissue showed α-SMA, VCAM-1,VLA-4,p-AKT,p-JNK,p-P38 were higher in the H358+CAFs group than in H358+NFs group, and decreased expression of VCAM-1,VLA-4,p-AKT,p-JNK,p-P38 in VCAM-1 antibody treatment group (Figure.6F). Taken together, in vivo data shown here support the view that VCAM-1 derived from CAFs promotes the growth and metastasis of lung cancer cell.

3.6 VCAM-1 secreted from CAFs has a poor prognosis in patients

To further investigate the correlations between VCAM-1 expression and the malignancy and prognosis of lung cancer patients, we investigated 264 lung cancer patients from the GEO dataset

(GSE30219), which contains both tumor gene expression patterns and patient clinical pathological data. The risk assessment data showed that a higher expression of VCAM-1, α-SMA, ITGA4(VLA-4α) and ITGB1(VLA-4β) exhibited a higher risk ($p < 0.001$) (Figure.7A, B, C, D). To analyze the relationship between α-SMA /VCAM-1, VCAM-1/ITGA4(VLA-4α), VCAM-1/ ITGB1(VLA-4β), the Pearson correlation results showed that these two molecules had a positive correlation ($p < 0.001$) (Figure.7 E, F, G). Of the 264 patients, 30 exhibited low levels of VCAM-1, and 234 remained at a high level. The difference of survival rate between the high VCAM-1 group and low VCAM-1 group was statistically significant ($p = 0.004563$) (Figure.7H). As shown in Table 2, the VCAM-1 expression was significantly correlated with cancer distinct metastasis. These data indicate that the VCAM-1 secreted from CAFs has a poor prognosis in patients and suggest the potential value of VCAM-1 as a prognostic biomarker and therapeutic target.

4. Discussion

Numerous evidence has demonstrated that CAFs play a critical role in cancer procession, including altering the immune response and inflammation, maintaining stemness and metabolism, inhibiting apoptosis, and enhancing proliferation, invasion and metastasis, and so on[29, 30]. Although some studies have found that CAFs are involved in the growth and metastasis of lung cancer[3, 14, 31], the role of CAFs in lung cancer and its mechanism have still not been fully elucidated. Here, we further confirm that CAFs increase the growth, migration and invasion of lung cancer cells in vitro and in vivo, and clarify the important role of CAFs in the microenvironment of lung cancer.

CAFs have been reported to secrete cytokines including growth factor, chemokine, and inflammatory factors to stimulate the signaling pathways and biological functions of cancer [11, 32]. Previous research has indicated that several cytokines were upregulated in CAFs and participated in promoting lung cancer growth and metastasis, such as IL-6, IL-22, HGF and TGF-β1[3, 14, 16, 33, 34]. In the present work, we identified a novel cytokine, VCAM-1, which is a transmembrane immunoglobulin and is considered to be a cell adhesion molecule, which was over-expressed in the supernatant of CAFs, blocking the expression of VCAM-1 in CAF-CM, and the proliferation and invasion of cancer cells co-cultured with CAF-CM was attenuated.

Meanwhile, from the screening results, we identified some differential expression cytokines, such as HGF, which—consistent with the previous reports—are secreted from CAFs and increased the expression and phosphorylation of ANXA2 and thus induced EMT and EGFR-TKI resistance in lung cancer[16]. However, we also observed that IL-6, which was highly secreted by CAFs and mediated chemoresistance in NSCLC by increasing EMT signaling in the previous reports[35], was not significant in our experiment. We consider that this difference between our results and the previous reports may be due to the origin of CAFs derived from diverse patients.

VCAM-1 is a member of the transmembrane immunoglobulin superfamily, which contains a cytoplasmic domain, a transmembrane region and several extracellular Ig-like domains. The extracellular domains one and four have been revealed as binding sites for VLA-4, which is the predominant receptor for VCAM-1[20]. VCAM-1 is known to exist as both a transmembrane protein and in a soluble form. The soluble form of VCAM-1, which generated from proteolytic cleaving of extracellular domains of full-length VCAM-1, still can bind to its ligands[23]. In tumorigenesis, a series of studies confirmed that VCAM-1 contributes to progress and metastasis in many cancers[26, 36-38]. However, the role of VCAM-1 in the tumor microenvironment of lung cancer has not been investigated. The current study showed that VCAM-1 secreted from CAFs enhances the proliferation, migration and invasion of lung cancer cells. Furthermore, the data from the animal experiment demonstrated that CAFs could increase the tumor volume of lung cancer cells in mice. A possibility should be noted that, in vivo experiments, the full-length VCAM-1 of CAFs can stimulate the growth and invasion of cancer cells adjacent to CAFs through cell attachment. Additionally, bioinformatics analysis indicated that VCAM-1 was associated with a poor prognosis in lung cancer patients.

One of the concerned problems is the molecular mechanism to cause the increase of soluble VCAM-1 in CAFs in this study. It has been found that NFs can be induced by some cytokines in tumor microenvironment, such as TGF-β, PDGF, bFGF, etc., which are secreted by tumor cells, resulting in up-regulation of a series of signaling pathways, such as NF-κB, ERK and Akt, and activated NFs into CAFs[5]. Interestingly, these pathways have been also shown to regulate VCAM-1 expression[39]. Therefore, we speculate that NFs under activation process by MAPK

and NF- κB signaling, probably simultaneously promotes the expression and secretion of VCAM-1 of the CAFs, which in turn promotes the tumorigenesis and metastasis of tumor cells. However, this meaningful question needs further study.

Previous studies have proved that VCAM-1 mediated cancer progress, mainly depending on the binding receptor VLA-4 and further activating numerous pathways[40, 41]. VCAM-1 triggers Akt activation via VLA-4 and provides a survival and metastasis advantage to breast cancer cells[24]. The VCAM-1/VLA-4 axis plays a key role in Wnt-induced secreted protein-1 (WISP-1) regulating the adhesion of prostate cancer cells to osteoblasts via the MAPK pathway, and matricellular protein SPARC-induced paracellular permeability is dependent on the endothelial VCAM-1 and p38 MAPK signaling in human pulmonary melanoma[25, 26]. The VLA-4-mediated upregulation of the Bcl-2/Bax ratio contributes to the anti-apoptotic effect in B cell chronic lymphocytic leukemia (B-CLL) cells[27]. Tumoral microvesicles (TMVs) transported VCAM-1 from melanoma cancer cells and promote the transformation of normal fibroblasts to tumor-associated fibroblasts by activating ERK1/2 via VLA-4[28]. In current study, the results showed that VCAM-1 secreted from CAF-CM and bound to the VLA-4 receptor, subsequently activated AKT, JNK and P38 in A549 and H358 cells. However, CAF-CM has no influence on Bcl-2. Meanwhile, the phosphorylation of ERK is variable in different lung cancer cells. These findings suggest that CAFs activate the AKT and MAPK signaling pathways in lung cancer cells via the VCAM-1/VLA-4 axis.

In summary, we found that VCAM-1 secreted from CAFs through binding with VLA-4 in cancer cells enhances the growth, migration and invasion of lung cancer by activating the MAPK and JNK pathway (Figure 7I). Our results provide a better understanding of how CAFs work in the tumor microenvironment in lung cancer, and VCAM-1 may be a novel drug target to inhibit cancer metastasis. Based on its active involvement in the progress of lung cancer cells, VCAM-1 may also serve as a predictive and prognostic biomarker.

Acknowledgements: This work was supported by the National Natural Science Foundation of China (Grant Nos. 81672761 and 81372182) and the Natural Science Foundation of Hunan

Province (2018JJ2545).

Conflicts of Interest: The authors declare no conflict of interest.

Reference:

[1] R.L. Siegel, K.D. Miller, A. Jemal, Cancer statistics, 2019, CA Cancer J Clin, 69 (2019) 7-34.
[2] A. Curioni-Fontecedro, L. Husmann, D. Soldini, R.A. Stahel, Primary non-small cell lung cancer response upon treatment with denosumab, Lung Cancer, 82 (2013) 506-508.
[3] L. Wang, L. Cao, H. Wang, B. Liu, Q. Zhang, Z. Meng, X. Wu, Q. Zhou, K. Xu, Cancer-associated fibroblasts enhance metastatic potential of lung cancer cells through IL-6/STAT3 signaling pathway, Oncotarget, 8 (2017) 76116-76128.
[4] D.F. Quail, J.A. Joyce, Microenvironmental regulation of tumor progression and metastasis, Nat Med, 19 (2013) 1423-1437.
[5] R. Kalluri, The biology and function of fibroblasts in cancer, Nat Rev Cancer, 16 (2016) 582-598.
[6] G. Ishii, A. Ochiai, S. Neri, Phenotypic and functional heterogeneity of cancer-associated fibroblast within the tumor microenvironment, Adv Drug Deliv Rev, 99 (2016) 186-196.
[7] Y. Mezawa, A. Orimo, The roles of tumor- and metastasis-promoting carcinoma-associated fibroblasts in human carcinomas, Cell Tissue Res, 365 (2016) 675-689.
[8] J. Paulsson, P. Micke, Prognostic relevance of cancer-associated fibroblasts in human cancer, Semin Cancer Biol, 25 (2014) 61-68.
[9] R.M. Bremnes, T. Donnem, S. Al-Saad, K. Al-Shibli, S. Andersen, R. Sirera, C. Camps, I. Marinez, L.T. Busund, The role of tumor stroma in cancer progression and prognosis: emphasis on carcinoma-associated fibroblasts and non-small cell lung cancer, J Thorac Oncol, 6 (2011) 209-217.
[10] J. Li, J. Guan, X. Long, Y. Wang, X. Xiang, mir-1-mediated paracrine effect of cancer-associated fibroblasts on lung cancer cell proliferation and chemoresistance, Oncol Rep, 35 (2016) 3523-3531.
[11] P. Gascard, T.D. Tlsty, Carcinoma-associated fibroblasts: orchestrating the composition of malignancy, Genes Dev, 30 (2016) 1002-1019.
[12] X. Yang, Y. Li, L. Zou, Z. Zhu, Role of Exosomes in Crosstalk Between Cancer-Associated Fibroblasts and Cancer Cells, Front Oncol, 9 (2019) 356.
[13] S. Vicent, L.C. Sayles, D. Vaka, P. Khatri, O. Gevaert, R. Chen, Y. Zheng, A.K. Gillespie, N. Clarke, Y. Xu, J. Shrager, C.D. Hoang, S. Plevritis, A.J. Butte, E.A. Sweet-Cordero, Cross-species functional analysis of cancer-associated fibroblasts identifies a critical role for CLCF1 and IL-6 in non-small cell lung cancer in vivo, Cancer Res, 72 (2012) 5744-5756.
[14] H. Li, Q. Zhang, Q. Wu, Y. Cui, H. Zhu, M. Fang, X. Zhou, Z. Sun, J. Yu, Interleukin-22 secreted by cancer-associated fibroblasts regulates the proliferation and metastasis of lung cancer cells via the PI3K-Akt-mTOR signaling pathway, Am J Transl Res, 11 (2019) 4077-4088.
[15] W.J. Chen, C.C. Ho, Y.L. Chang, H.Y. Chen, C.A. Lin, T.Y. Ling, S.L. Yu, S.S. Yuan, Y.J. Chen, C.Y. Lin, S.H. Pan, H.Y. Chou, Y.J. Chen, G.C. Chang, W.C. Chu, Y.M. Lee, J.Y. Lee, P.J. Lee, K.C. Li, H.W. Chen, P.C. Yang, Cancer-associated fibroblasts regulate the plasticity of lung cancer stemness via paracrine signalling, Nat Commun, 5 (2014) 3472.
[16] Y. Yi, S. Zeng, Z. Wang, M. Wu, Y. Ma, X. Ye, B. Zhang, H. Liu, Cancer-associated fibroblasts promote epithelial-mesenchymal transition and EGFR-TKI resistance of non-small cell lung cancers via

HGF/IGF-1/ANXA2 signaling, Biochim Biophys Acta Mol Basis Dis, 1864 (2018) 793-803.
[17] J. You, M. Li, L.M. Cao, Q.H. Gu, P.B. Deng, Y. Tan, C.P. Hu, Snail1-dependent cancer-associated fibroblasts induce epithelial-mesenchymal transition in lung cancer cells via exosomes, QJM, 112 (2019) 581-590.
[18] J. You, M. Li, Y. Tan, L. Cao, Q. Gu, H. Yang, C. Hu, Snail1-expressing cancer-associated fibroblasts induce lung cancer cell epithelial-mesenchymal transition through miR-33b, Oncotarget, 8 (2017) 114769-114786.
[19] J. Liu, S. Chen, W. Wang, B.F. Ning, F. Chen, W. Shen, J. Ding, W. Chen, W.F. Xie, X. Zhang, Cancer-associated fibroblasts promote hepatocellular carcinoma metastasis through chemokine-activated hedgehog and TGF-beta pathways, Cancer Lett, 379 (2016) 49-59.
[20] X. Lu, E. Mu, Y. Wei, S. Riethdorf, Q. Yang, M. Yuan, J. Yan, Y. Hua, B.J. Tiede, X. Lu, B.G. Haffty, K. Pantel, J. Massague, Y. Kang, VCAM-1 promotes osteolytic expansion of indolent bone micrometastasis of breast cancer by engaging alpha4beta1-positive osteoclast progenitors, Cancer Cell, 20 (2011) 701-714.
[21] S. Rousseaux, A. Debernardi, B. Jacquiau, A.L. Vitte, A. Vesin, H. Nagy-Mignotte, D. Moro-Sibilot, P.Y. Brichon, S. Lantuejoul, P. Hainaut, J. Laffaire, A. de Reynies, D.G. Beer, J.F. Timsit, C. Brambilla, E. Brambilla, S. Khochbin, Ectopic activation of germline and placental genes identifies aggressive metastasis-prone lung cancers, Sci Transl Med, 5 (2013) 186ra166.
[22] N. Sampson, E. Brunner, A. Weber, M. Puhr, G. Schafer, C. Szyndralewiez, H. Klocker, Inhibition of Nox4-dependent ROS signaling attenuates prostate fibroblast activation and abrogates stromal-mediated protumorigenic interactions, Int J Cancer, 143 (2018) 383-395.
[23] M. Schlesinger, G. Bendas, Vascular cell adhesion molecule-1 (VCAM-1)--an increasing insight into its role in tumorigenicity and metastasis, Int J Cancer, 136 (2015) 2504-2514.
[24] Q. Chen, X.H. Zhang, J. Massague, Macrophage binding to receptor VCAM-1 transmits survival signals in breast cancer cells that invade the lungs, Cancer Cell, 20 (2011) 538-549.
[25] A.C. Chang, P.C. Chen, Y.F. Lin, C.M. Su, J.F. Liu, T.H. Lin, S.M. Chuang, C.H. Tang, Osteoblast-secreted WISP-1 promotes adherence of prostate cancer cells to bone via the VCAM-1/integrin alpha4beta1 system, Cancer Lett, 426 (2018) 47-56.
[26] M. Tichet, V. Prod'Homme, N. Fenouille, D. Ambrosetti, A. Mallavialle, M. Cerezo, M. Ohanna, S. Audebert, S. Rocchi, D. Giacchero, F. Boukari, M. Allegra, J.C. Chambard, J.P. Lacour, J.F. Michiels, J.P. Borg, M. Deckert, S. Tartare-Deckert, Tumour-derived SPARC drives vascular permeability and extravasation through endothelial VCAM1 signalling to promote metastasis, Nat Commun, 6 (2015) 6993.
[27] M.T. de la Fuente, B. Casanova, M. Garcia-Gila, A. Silva, A. Garcia-Pardo, Fibronectin interaction with alpha4beta1 integrin prevents apoptosis in B cell chronic lymphocytic leukemia: correlation with Bcl-2 and Bax, Leukemia, 13 (1999) 266-274.
[28] X.P. Zhao, M. Wang, Y. Song, K. Song, T.L. Yan, L. Wang, K. Liu, Z.J. Shang, Membrane microvesicles as mediators for melanoma-fibroblasts communication: roles of the VCAM-1/VLA-4 axis and the ERK1/2 signal pathway, Cancer Lett, 360 (2015) 125-133.
[29] M. Wang, J. Zhao, L. Zhang, F. Wei, Y. Lian, Y. Wu, Z. Gong, S. Zhang, J. Zhou, K. Cao, X. Li, W. Xiong, G. Li, Z. Zeng, C. Guo, Role of tumor microenvironment in tumorigenesis, J Cancer, 8 (2017) 761-773.
[30] K.A. Gieniec, L.M. Butler, D.L. Worthley, S.L. Woods, Cancer-associated fibroblasts-heroes or villains?, Br J Cancer, 121 (2019) 293-302.
[31] T. Yu, Z. Guo, H. Fan, J. Song, Y. Liu, Z. Gao, Q. Wang, Cancer-associated fibroblasts promote

non-small cell lung cancer cell invasion by upregulation of glucose-regulated protein 78 (GRP78) expression in an integrated bionic microfluidic device, Oncotarget, 7 (2016) 25593-25603.
[32] L. Bu, H. Baba, N. Yoshida, K. Miyake, T. Yasuda, T. Uchihara, P. Tan, T. Ishimoto, Biological heterogeneity and versatility of cancer-associated fibroblasts in the tumor microenvironment, Oncogene, 38 (2019) 4887-4901.
[33] Y. Ren, H.H. Jia, Y.Q. Xu, X. Zhou, X.H. Zhao, Y.F. Wang, X. Song, Z.Y. Zhu, T. Sun, Y. Dou, W.P. Tian, X.L. Zhao, C.S. Kang, M. Mei, Paracrine and epigenetic control of CAF-induced metastasis: the role of HOTAIR stimulated by TGF-ss1 secretion, Mol Cancer, 17 (2018) 5.
[34] W. Wang, Q. Li, T. Yamada, K. Matsumoto, I. Matsumoto, M. Oda, G. Watanabe, Y. Kayano, Y. Nishioka, S. Sone, S. Yano, Crosstalk to stromal fibroblasts induces resistance of lung cancer to epidermal growth factor receptor tyrosine kinase inhibitors, Clin Cancer Res, 15 (2009) 6630-6638.
[35] Y. Shintani, A. Fujiwara, T. Kimura, T. Kawamura, S. Funaki, M. Minami, M. Okumura, IL-6 Secreted from Cancer-Associated Fibroblasts Mediates Chemoresistance in NSCLC by Increasing Epithelial-Mesenchymal Transition Signaling, J Thorac Oncol, 11 (2016) 1482-1492.
[36] O. Dorr, C. Liebetrau, H. Mollmann, L. Gaede, C. Troidl, J. Rixe, C. Hamm, H. Nef, Soluble fms-like tyrosine kinase-1 and endothelial adhesion molecules (intercellular cell adhesion molecule-1 and vascular cell adhesion molecule-1) as predictive markers for blood pressure reduction after renal sympathetic denervation, Hypertension, 63 (2014) 984-990.
[37] R. Sharma, R. Sharma, T.P. Khaket, C. Dutta, B. Chakraborty, T.K. Mukherjee, Breast cancer metastasis: Putative therapeutic role of vascular cell adhesion molecule-1, Cell Oncol (Dordr), 40 (2017) 199-208.
[38] S. Cheng, Z. Li, J. He, S. Fu, Y. Duan, Q. Zhou, Y. Yan, X. Liu, L. Liu, C. Feng, L. Zhang, J. He, Y. Deng, L.Q. Sun, Epstein-Barr virus noncoding RNAs from the extracellular vesicles of nasopharyngeal carcinoma (NPC) cells promote angiogenesis via TLR3/RIG-I-mediated VCAM-1 expression, Biochim Biophys Acta Mol Basis Dis, 1865 (2019) 1201-1213.
[39] D.H. Kong, Y.K. Kim, M.R. Kim, J.H. Jang, S. Lee, Emerging Roles of Vascular Cell Adhesion Molecule-1 (VCAM-1) in Immunological Disorders and Cancer, Int J Mol Sci, 19 (2018).
[40] M. Schlesinger, G. Bendas, Contribution of very late antigen-4 (VLA-4) integrin to cancer progression and metastasis, Cancer Metastasis Rev, 34 (2015) 575-591.
[41] R. Jacamo, Y. Chen, Z. Wang, W. Ma, M. Zhang, E.L. Spaeth, Y. Wang, V.L. Battula, P.Y. Mak, K. Schallmoser, P. Ruvolo, W.D. Schober, E.J. Shpall, M.H. Nguyen, D. Strunk, C.E. Bueso-Ramos, S. Konoplev, R.E. Davis, M. Konopleva, M. Andreeff, Reciprocal leukemia-stroma VCAM-1/VLA-4-dependent activation of NF-kappaB mediates chemoresistance, Blood, 123 (2014) 2691-2702.

Table 1. Primers used in this study

Gene	Forward sequence (5’ to 3’)	Reverse sequence (5’ to 3’)
Actin	CTACCTCATGAAGATCCTCACC	AGTTGAAGGTAGTTTCGTGGAT
TBSN	GGCACCAACCGCATTCCAGAG	GCACAGCATCCACCAGGTCTTG
VEGF	GCCTTGCCTTGCTGCTCTACC	AGACATCCATGAACTTCACCACTTCG
VCAM-1	ACCACATCTACGCTGACAATGAATCC	AACACTTGACTGTGATCGGCTTCC
SDF-1	TCGTGGTCGTGCTGGTCCTC	TTGAGATGCTTGACGTTGGCTCTG
MIF	GCAGAACCGCTCCTACAGCAAG	TGGCCGCGTTCATGTCGTAATAG
IGFBP-3	ACTACGAGTCTCAGAGCACAGATACC	AGCACATTGAGGAACTTCAGGTGATTC
IGFBP-2	AACAGTGCAAGATGTCTCTGAACGG	GCCTCCTGCTGCTCATTGTAGAAG
HGF	TCCAAGGTCAAGGAGAAGGCTACAG	GAGTCATGTCATGCTCGTGAGGATAC
CD147	GCCTGGTACAAGATCACTGACTCTG	CTGCGAGGAACTCACGAAGAACC
Cystatin C	GGTGAACTACTTCTTGGACGTGGAG	CAGATGTGGCTGGTCATGGAAGG
Angiogenin	GGCAACAAGCGCAGCATCAAG	TGGCTCGGTACTGGCATGGAG
VLA-4	CTGTGATGCCTTACATTAGCAC	ATCCAAATTTCCAGATATGCGC

Table2: Clinicopathologic Characteristics and VCAM-1 expression of the study patients

Clinic pathology		High VCAM-1 N (%)	Low VCAM-1 N (%)	P
Gender	Male	199(89.24)	24(10.76)	0.4728
	Female	35(85.37)	6(14.63)	
Age	<60	93(84.55)	17(15.45)	0.1145[a]
	≥60	140(90.50)	13(8.50)	
Tumor stage	T1-T2	191(87.61)	27(12.39)	0.1305[b]
	T3-T4	42(95.45)	2(4.55)	
Regional Lymph Nodes stage	N0	167(88.36)	22(11.64)	0.6352[b]
	N1-N3	66(90.41)	7(9.59)	
Distant Metastasis stage	M0	230(89.49)	27(10.51)	0.0126*[c]
	M1-M3	2(50)	2(50)	

[a] The clinic pathology of one patient is unknow; [b] The clinic pathology of two patients is unknow; [c] The clinic pathology of three patients is unknow.

P value represents the probability from a chi-square test for VCAM-1 levels between variable subgroups. *P < 0.05

Abbreviations: VCAM-1, Vascular Cell Adhesion Molecule-1；

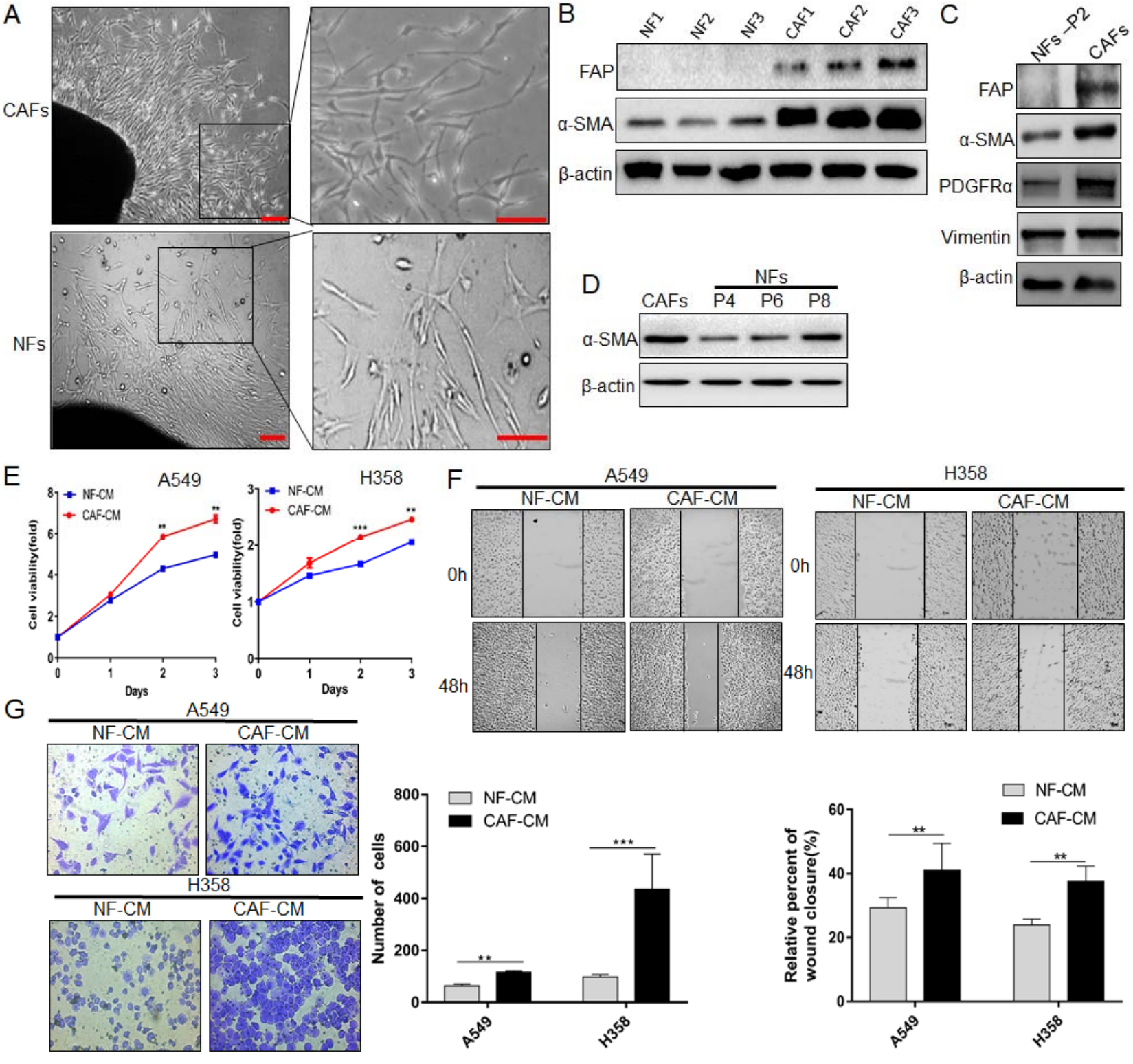
A
CAFs
NFs
B
NF1
NF2
NF3
CAF1
CAF2
CAF3
FAP
α-SMA
β-actin
C
NFs –P2
CAFs
FAP
α-SMA
PDGFRα
Vimentin
β-actin
D
NFs
CAFs
P4
P6
P8
α-SMA
β-actin
E
A549
H358
NF-CM
CAF-CM
Cell viability(fold)
Days
F
A549
H358
NF-CM
CAF-CM
0h
48h
G
A549
H358
NF-CM
CAF-CM
Number of cells
Relative percent of wound closure(%)

A

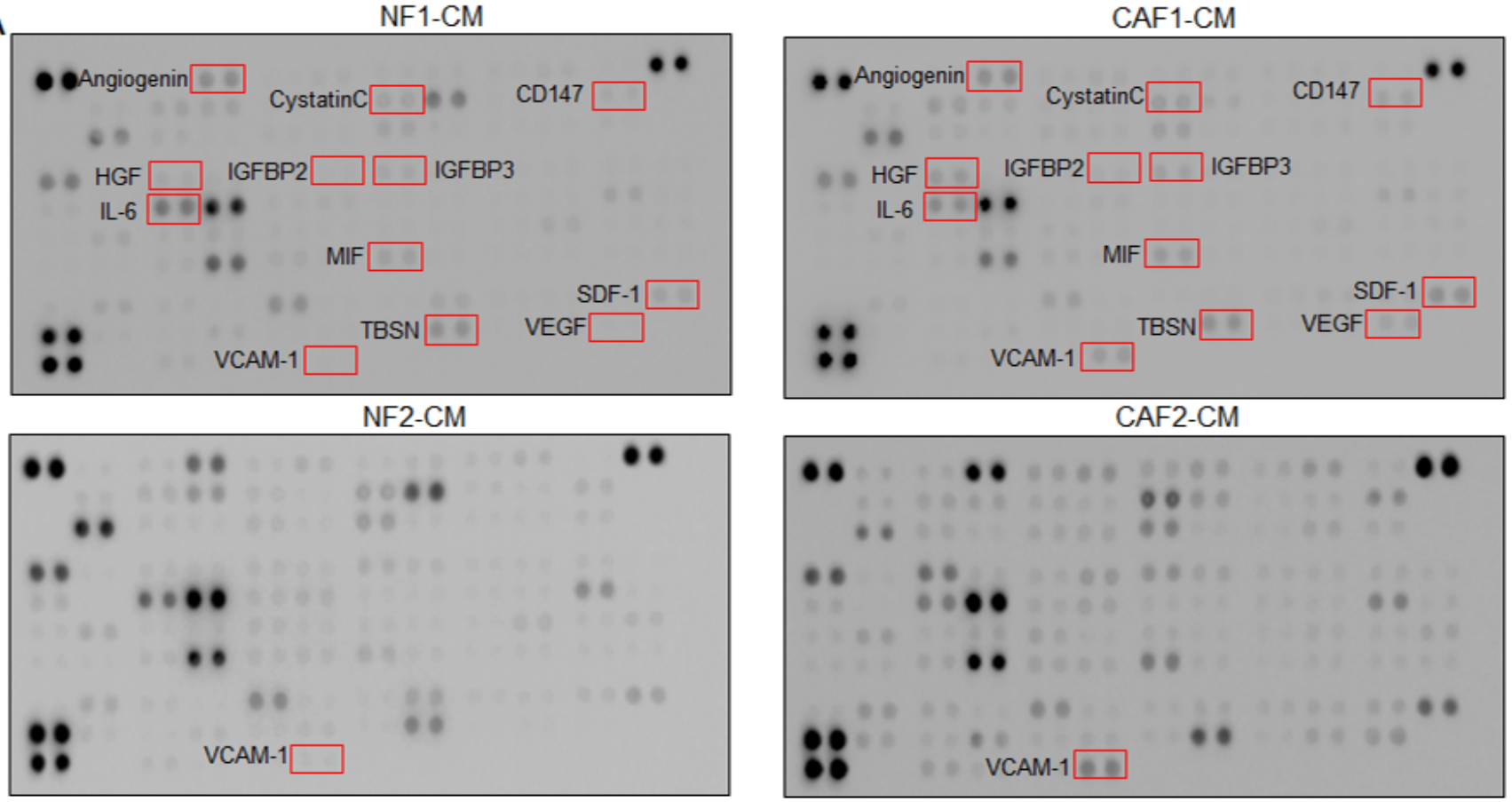

B

Cytokine	NF-CM	CAF-CM	P-value
Angiogenin	5382 ± 105.6	8046 ± 13.35	< 0.01
CystatinC	1745 ± 12.42	4088 ± 27.76	< 0.01
CD147	655.9 ± 20.55	1540 ± 65.53	< 0.01
HGF	625.8 ± 50.50	2994 ± 46.78	< 0.001
IGFBP-2	494.3 ± 28.59	1015 ± 19.42	< 0.01
IGFBP-3	848.4 ± 11.48	1226 ± 1.206	< 0.01
MIF	1121 ± 50.95	2359 ± 29.79	< 0.01
SDF-1	1443 ± 109.6	3361 ± 10.03	< 0.01
TBSN	3832 ± 71.98	4588 ± 30.85	< 0.01
VEGF	66.91 ± 25.45	1149 ± 103.4	< 0.001
VCAM-1	327.9 ± 25.41	2282 ± 50.68	< 0.001
IL-6	1047 ± 236.73	1095 ± 37.15	NS

C

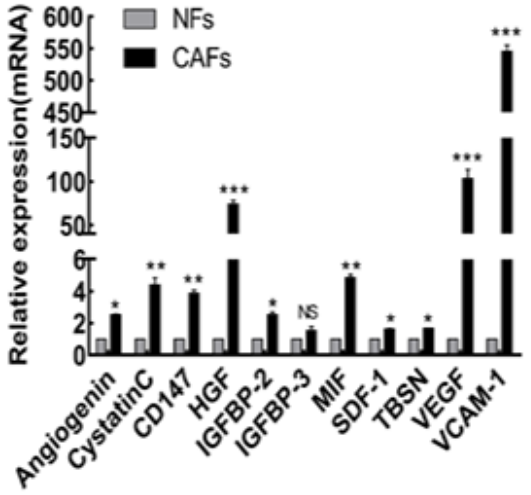

D

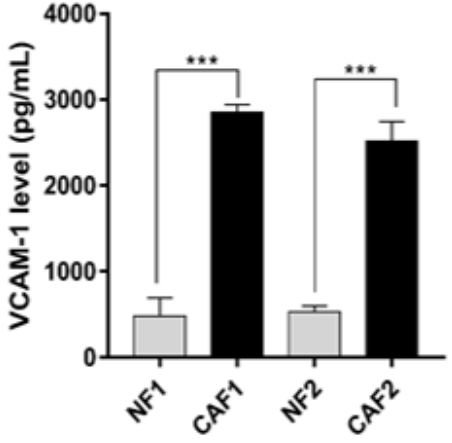

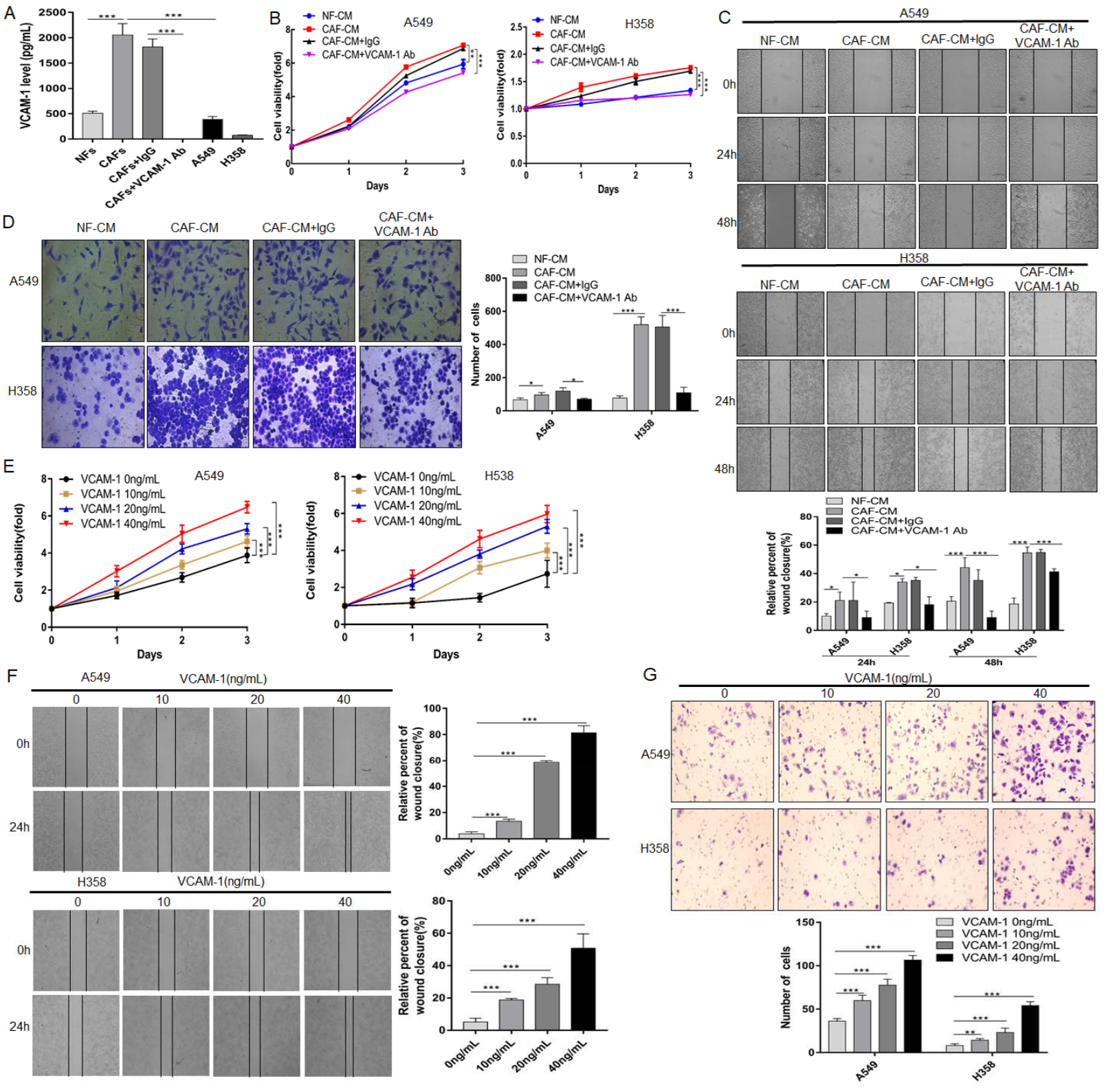
A
VCAM-1 level (pg/mL)
NFs
CAFs
CAFs+IgG
CAFs+VCAM-1 Ab
A549
H358
B
A549
H358
NF-CM
CAF-CM
CAF-CM+IgG
CAF-CM+VCAM-1 Ab
Cell viability(fold)
Days
C
A549
H358
NF-CM
CAF-CM
CAF-CM+IgG
CAF-CM+ VCAM-1 Ab
0h
24h
48h
Relative percent of wound closure(%)
24h
48h
D
A549
H358
Number of cells
E
A549
H538
VCAM-1 0ng/mL
VCAM-1 10ng/mL
VCAM-1 20ng/mL
VCAM-1 40ng/mL
F
A549
H358
VCAM-1(ng/mL)
0
10
20
40
0ng/mL
10ng/mL
20ng/mL
40ng/mL
G
VCAM-1(ng/mL)
Number of cells

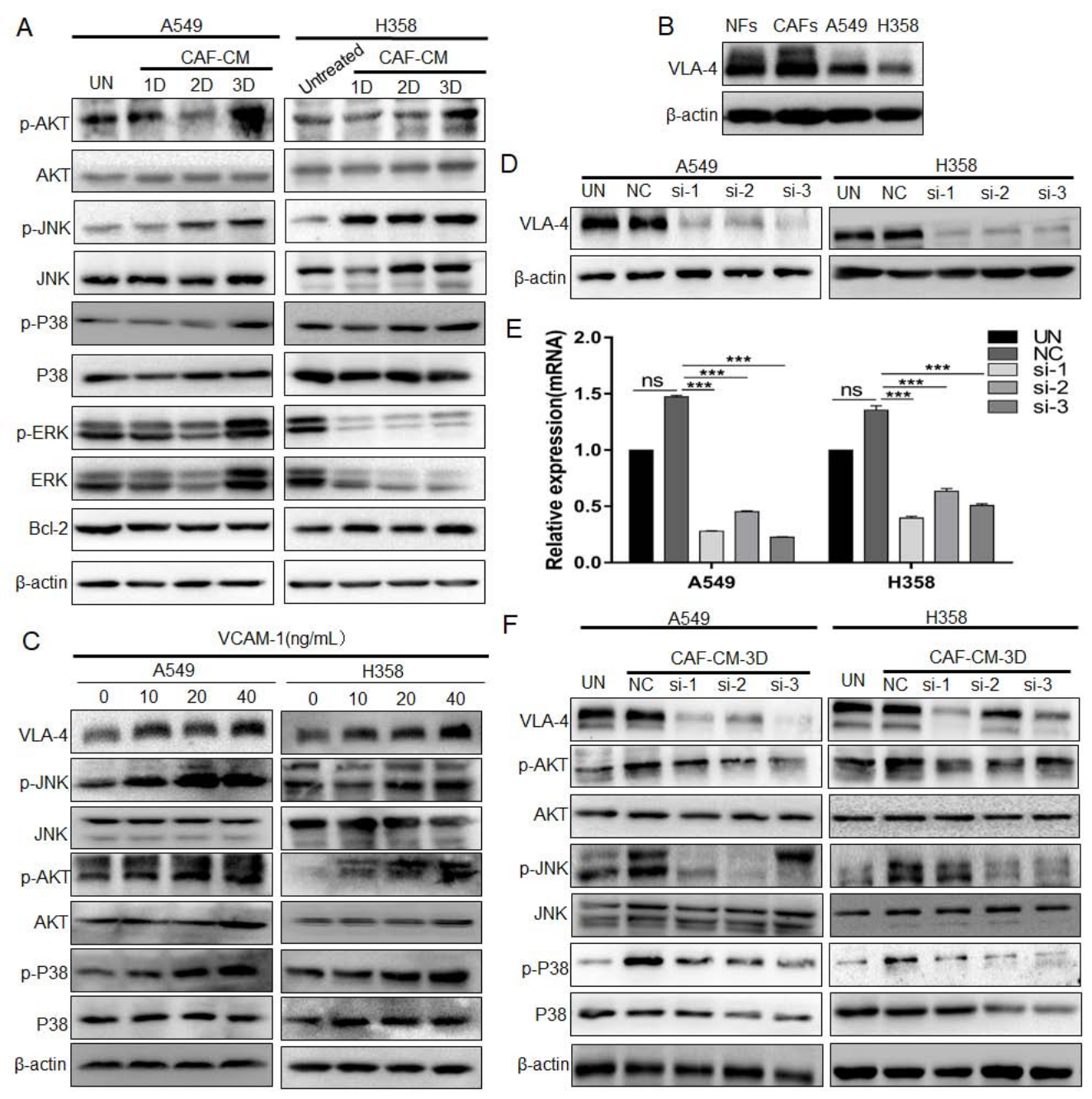
A
A549
H358
CAF-CM
UN
1D
2D
3D
Untreated
p-AKT
AKT
p-JNK
JNK
p-P38
P38
p-ERK
ERK
Bcl-2
β-actin
B
NFs
CAFs
A549
H358
VLA-4
β-actin
C
VCAM-1(ng/mL)
0
10
20
40
VLA-4
p-JNK
JNK
p-AKT
AKT
p-P38
P38
β-actin
D
UN
NC
si-1
si-2
si-3
VLA-4
β-actin
E
Relative expression(mRNA)
2.0
1.5
1.0
0.5
0.0
ns
***
A549
H358
F
CAF-CM-3D
VLA-4
p-AKT
AKT
p-JNK
JNK
p-P38
P38
β-actin

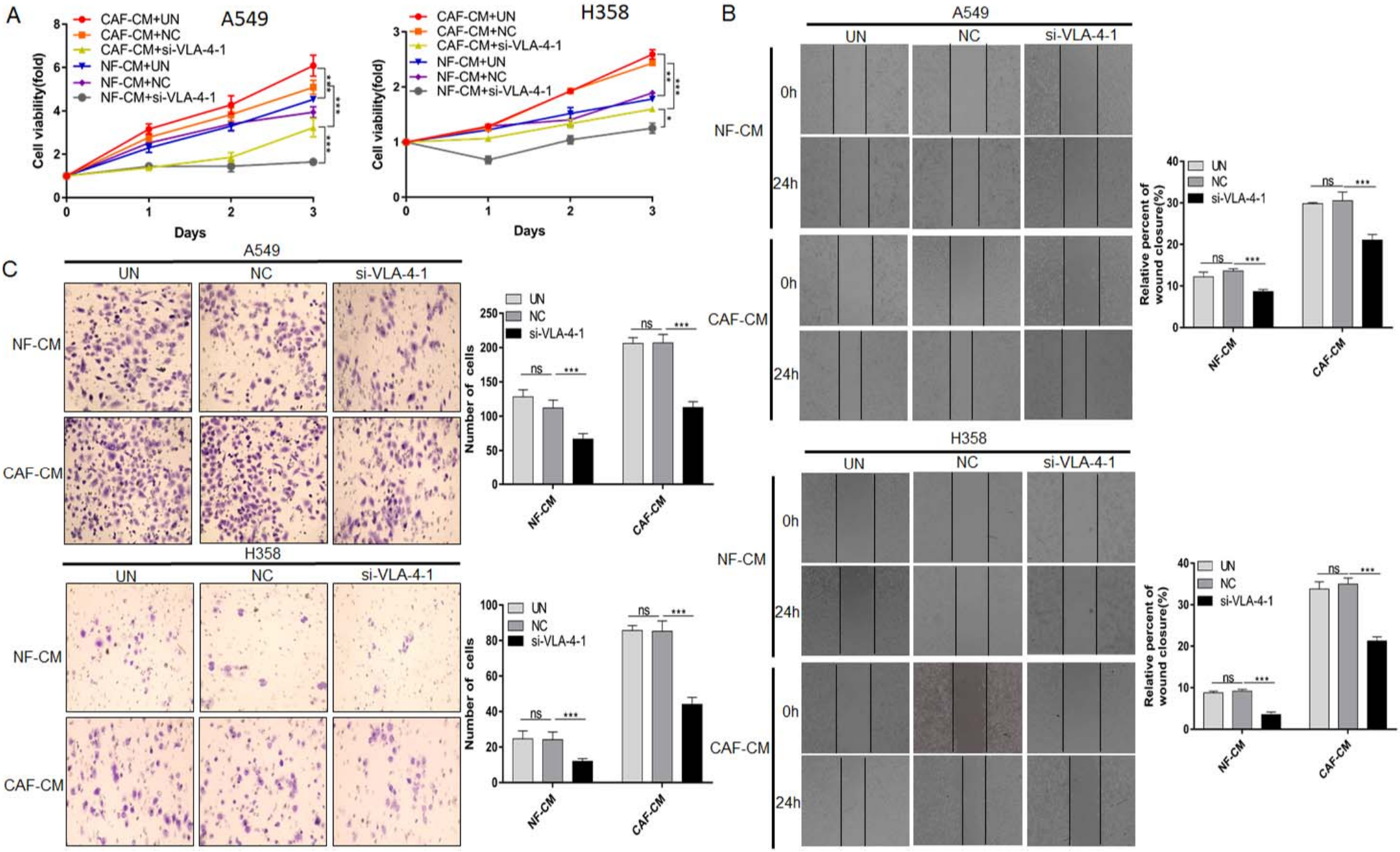
A
A549
H358
CAF-CM+UN
CAF-CM+NC
CAF-CM+si-VLA-4-1
NF-CM+UN
NF-CM+NC
NF-CM+si-VLA-4-1
Cell viability(fold)
Days
B
A549
H358
UN
NC
si-VLA-4-1
NF-CM
CAF-CM
0h
24h
Relative percent of wound closure(%)
C
A549
H358
Number of cells
ns
***

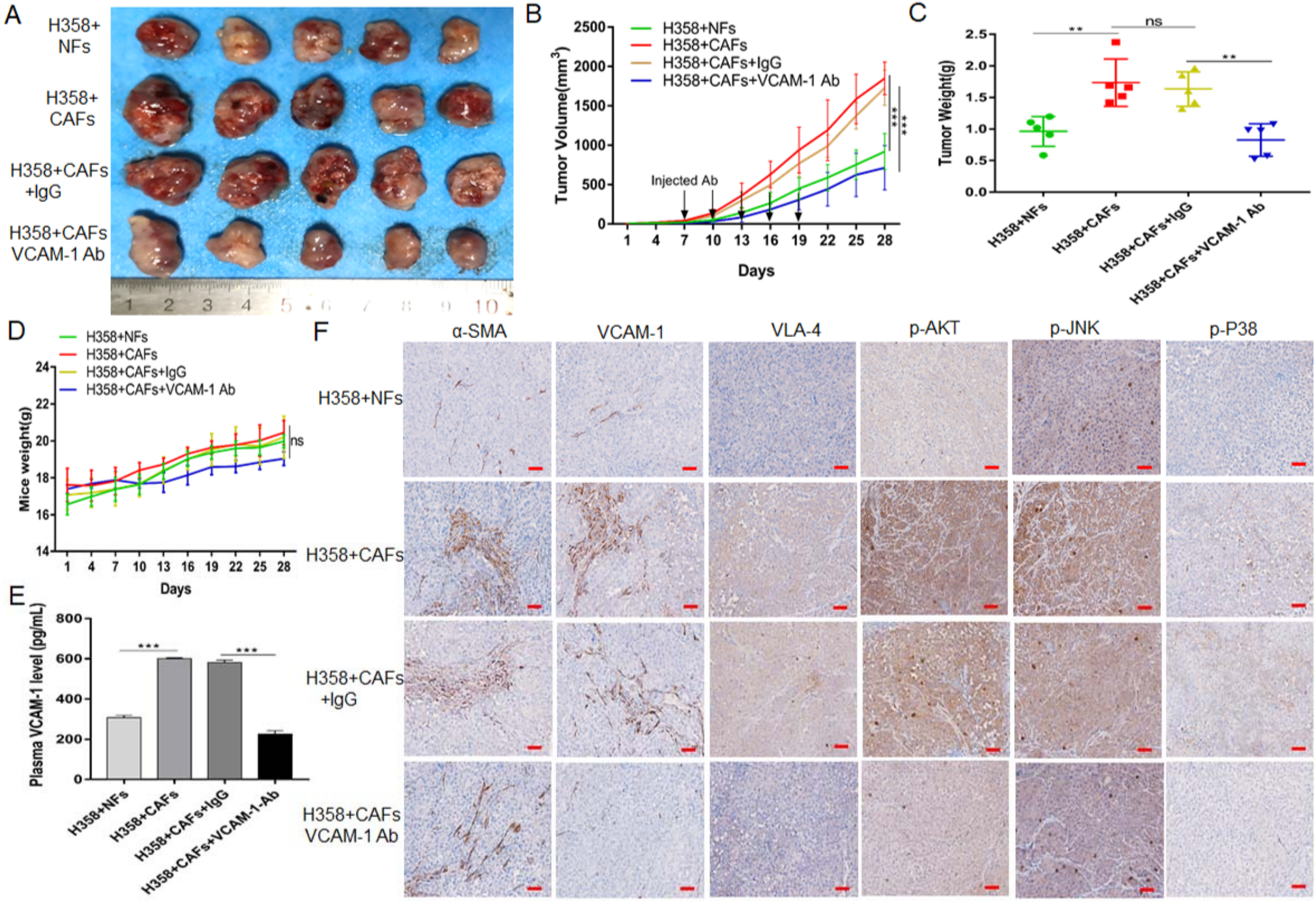
A
H358+ NFs
H358+ CAFs
H358+CAFs +IgG
H358+CAFs VCAM-1 Ab
B
H358+NFs
H358+CAFs
H358+CAFs+IgG
H358+CAFs+VCAM-1 Ab
Tumor Volume(mm3)
Injected Ab
Days
C
Tumor Weight(g)
ns
H358+NFs
H358+CAFs
H358+CAFs+IgG
H358+CAFs+VCAM-1 Ab
D
Mice weight(g)
ns
Days
E
Plasma VCAM-1 level (pg/mL)
F
α-SMA
VCAM-1
VLA-4
p-AKT
p-JNK
p-P38
H358+NFs
H358+CAFs
H358+CAFs +IgG
H358+CAFs VCAM-1 Ab

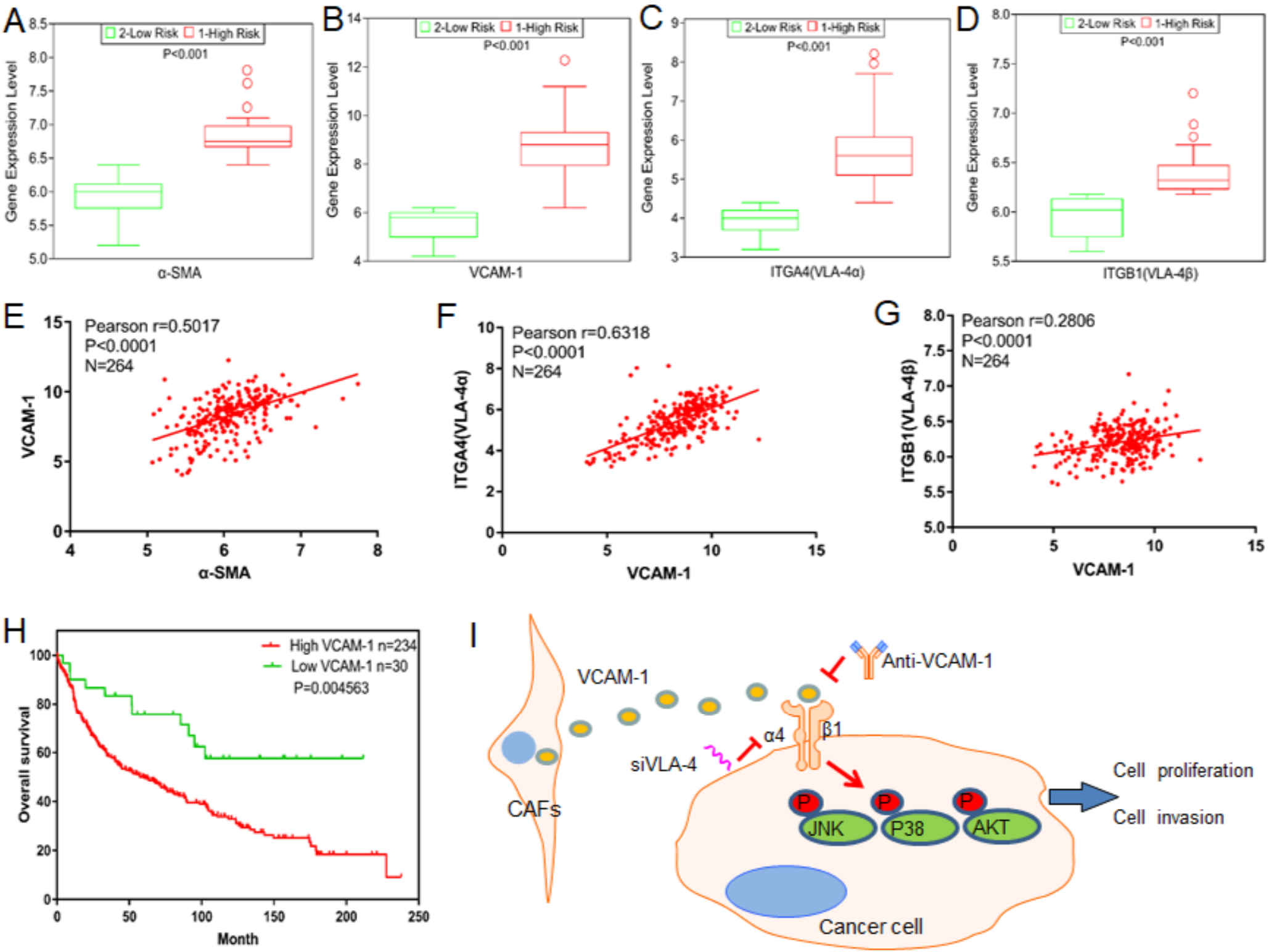
A
2-Low Risk
1-High Risk
P<0.001
Gene Expression Level
α-SMA
B
2-Low Risk
1-High Risk
P<0.001
Gene Expression Level
VCAM-1
C
2-Low Risk
1-High Risk
P<0.001
Gene Expression Level
ITGA4(VLA-4α)
D
2-Low Risk
1-High Risk
P<0.001
Gene Expression Level
ITGB1(VLA-4β)
E
Pearson r=0.5017
P<0.0001
N=264
VCAM-1
α-SMA
F
Pearson r=0.6318
P<0.0001
N=264
ITGA4(VLA-4α)
VCAM-1
G
Pearson r=0.2806
P<0.0001
N=264
ITGB1(VLA-4β)
VCAM-1
H
High VCAM-1 n=234
Low VCAM-1 n=30
P=0.004563
Overall survival
Month
I
VCAM-1
Anti-VCAM-1
α4
β1
siVLA-4
CAFs
P
JNK
P38
AKT
Cell proliferation
Cell invasion
Cancer cell

Figure legends

Fig.1. The conditional medium (CM) of cancer-associated fibroblasts (CAFs) promotes the proliferation, migration and invasion of recipient lung cancer cells. (A) The representative microscope images of primary culture cells CAFs and normal fibroblasts (NFs) isolated from lung cancer tissues. Scale bar, 100 μm. (B) Western blot analysis of the CAF marker protein alpha-smooth muscle actin (α-SMA) and fibroblast-activated protein (FAP) in three pairs of primary cells. (C) Western blot analysis of the CAF marker protein α-SMA, FAP, platelet-derived growth factor receptor-alpha (PDGFRα) and the mesenchyme marker Vimentin. (D) Western blot analysis for α-SMA in the increasing generation of NFs. (E-G) Cancer cells cultured with CAF-conditional medium (CM) or NF-CM. (E) MTS assay was used to analyze the cell proliferation of A549 and H358 cells. (F) Cell motility ability was measured by wound healing assay in A549 and H358 cells. The percentage of wound closure was determined at 48 hours; representative photographs are presented (×40 magnification). (G) Cell invasion was measured by the transwell assay in A549 and H358 cells after 48 hours; representative photographs are presented (×200 magnification). Results are presented as the mean ± SD of three independent experiments. **p < 0.01, ***p < 0.001.

Fig.2. Identification of differentially secreted cytokines between CAF-CM and NF-CM. (A) Representative cytokine arrays for the supernatant of NFs and CAFs. The cytokines with significant changes are marked with a square frame. (B) The statistical analysis of the gray-scale of 12 selected cytokines in CAFs and NFs are listed. The quantitative analysis of protein spots was performed using ImageJ software. (C) Quantitative RT-PCR quantified the expression of 11 cytokines in CAFs and NFs. (D) Soluble VCAM-1 in the supernatant of two pairs of primary cell NFs and CAFs was detected using ELISA. Results are presented as the mean ± SD of three independent experiments. *p < 0.05, **p < 0.01, ***p < 0.001, ns: not significant.

Fig.3. CAFs promote the proliferation, migration and invasion of lung cancer cells via the secretion of VCAM-1. (A) Soluble VCAM-1 was measured by ELISA in the supernatant of NFs, CAFs, CAFs treated with IgG or VCAM-1 neutralization antibody (5ug/ul) and A549 and H358 cells. (B-D) Cancer cells cultured with CAF-CM, NF-CM, CAF-CM+IgG and VCAM-1

neutralization antibody (5ug/ul), respectively. (B) MTS assay was performed to examine the proliferation ability of A549 and H358 cells after blocking the VCAM-1 of CAF-CM. (C) Cell motility ability was measured by wound healing assay in A549 and H358 cells after blocking the VCAM-1 of CAF-CM. The percentage of wound closure was, respectively, determined at 24 hours and 48 hours after blocking the VCAM-1 of CAF-CM, representative photographs are presented (×40 magnification). (D) Cell invasion was measured by the transwell assay in A549 and H358 cells after 48 hours; representative photographs are presented (×200 magnification). (E-G) Cancer cells cultured with different concentrations of recombinant human VCAM-1. (E) MTS assay was performed to examine the proliferation ability of A549 and H358 cells. (F) Cell motility ability was measured by wound healing assay in A549 and H358 cells after 24 hours, representative photographs are presented (×40 magnification). (G) Cell invasion was measured by the transwell assay in A549 and H358 cells after 48 hours, representative photographs are presented (×200 magnification). Results are presented as the mean ±SD of three independent experiments. *$p < 0.05$, **$p < 0.01$, ***$p < 0.001$, ns: not significant.

Fig.4. CAF-derived VCAM-1 activates the AKT, JNK and P38 pathway via receptor very-late antigen (VLA)-4. (A) Western blot analyzed several pathways correlated with VCAM-1 that promote the migration and invasion of lung cancer cells. (B) Western blot analyzed the protein expression of VLA-4 in NFs, CAFs, A549 and H358 cells. (C) Western blot analysis of AKT, JNK and P38 in lung cancer cell after treatment with recombinant human VCAM-1 for 3 days. (D) Western blot analyzed the expression of VLA-4 after siRNA treatment. (E) Quantitative RT-PCR was used to test the effect of three siRNAs in A549 and H358 cells. **$p < 0.01$, ***$p < 0.001$, ns: not significant. (F) Western blot analyzed the expression of AKT, JNK and P38 after VLA-4 inhibition in A549 and H358 cells cultured with CAF-CM for 3 days. UN, untreated; NC, negative control.

Fig.5. VLA-4 is required for CAF-CM promotes the lung cancer proliferation, invasion and migration

After cancer cell was transfected with siRNA targeting VLA-4 for 24 hours. (A) MTS assay analyzed the proliferation ability of A549 and H358 cells cultured with CAF-CM or NF-CM. (B)

Cell motility ability was measured by wound healing assay in A549 and H358 cells cocultured with NF-CM and CAF-CM. The percentage of wound closure was determined after 24 hours, representative photographs are presented (×40 magnification). (C) Cell invasion was measured by the transwell assay in A549 and H358 cells with NF-CM and CAF-CM treatment after 48 hours, representative photographs are presented (×200 magnification). Results are presented as the mean ±SD of three independent experiments. UN, untreated; NC, negative control. *p < 0.05, **p < 0.01, ***p < 0.001, ns: not significant.

Fig.6. VCAM-1 secreted from CAFs enhances tumor growth in vivo. (A) At the experimental end point, tumor xenografts were dissected and photographed. (B) Tumor volume was measured every 3 days after injection of tumor cells. Intratumoral injection of IgG or VCAM-1 neutralization antibody were performed after the tumor volume reaching to 60-80 mm^3. (C) Tumor weight was measured at the experimental end point. (D) The mice weight was measured at the experimental end point. (E) VCAM-1 levels in plasma from the tumor-bearing mice were measured using ELISA. (F) Representative immunohistochemistry (IHC) staining of α-SMA, VCAM-1, VLA-4, p-AKT, p-JNK, p-P38 expression of H358 xenografts in groups indicated in (A). Scale bar, 200 μm. *p < 0.05, **p < 0.01, ***p < 0.001, ns: not significant.

Fig.7. VCAM-1 derived from CAFs has a poor prognosis in patients. (A, B, C, D) The risk analysis in relation to α-SMA, VCAM-1, ITGA4 (VLA-4α) and ITGB1(VLA-4β) expression from GEO datasets, respectively. (E, F, G) Correlation between α-SMA and VCAM-1, VCAM-1 and ITGA4 (VLA-4α), and VCAM-1 and ITGB1(VLA-4β) expression levels in the lung cancer tissues (n = 264) were estimated by the Pearson correlation analysis, respectively. (H) Overall survival rates of lung cancer patients with low (n = 30) or high (n = 234) expression levels of VCAM-1 were estimated with the Kaplan–Meier method by log-rank test. (I) A schematic model shows that VCAM-1 secreted by CAFs is identified as a microenvironment modifier for lung cancer progression.

Highlights

·Vascular cell adhesion molecule-1 (VCAM-1) secreted from cancer associated fibroblasts (CAFs) promotes lung cancer cells proliferation, migration and invasion.

·CAFs activated AKT and MAPK signaling via VCAM-1 receptor α4β1 integrin (very-late antigen (VLA)-4) in lung cancer cells.

·VCAM-1 expression was associated with a poor prognosis in lung cancer patients.

Conflicts of Interest: The authors declare no conflict of interest.